Verification and Biophysical Characterization of a New Three-Color *Förster* Resonance-Energy-Transfer (FRET) System in DNA

by **Andrea Altevogt née Kienzler**[a]), **Roman Flehr**[b]), **Sören Gehne**[b]), **Michael U. Kumke**[b]), and **Willi Bannwarth***[a])

[a]) Albert-Ludwigs University of Freiburg, Institute of Organic Chemistry and Biochemistry, Albertstr. 21, D-79104 Freiburg (phone: +49-761-2036073; fax: +49-761-2038705; e-mail: willi.bannwarth@chemie.uni-freiburg.de)

[b]) University of Potsdam, Institute of Chemistry (Physical Chemistry), Karl-Liebknecht-Str. 24–25, D-14476 Potsdam-Golm

We report on a new three-color FRET system consisting of three fluorescent dyes, *i.e.*, of a carbostyril (=quinolin-2(1*H*)-one)-derived donor D, a (bathophenanthroline)ruthenium complex as a relay chromophore A_1, and a Cy dye as A_2 (FRET = *Förster* resonance-energy-transfer) (*cf. Fig. 1*). With their widely matching spectroscopic properties (*cf. Fig. 2*), the combination of these dyes yielded excellent FRET efficiencies. Furthermore, fluorescence lifetime measurements revealed that the long fluorescence lifetime of the Ru complex was transferred to the Cy dye offering the possibility to measure the whole system in a time-resolved mode. The FRET system was established on double-stranded DNA (*cf. Fig. 3*) but it should also be generally applicable to other biomolecules.

Introduction. – For the elucidation of distance-dependent biochemical events *Förster* resonance-energy-transfer (FRET) systems have emerged as powerful tools, since they allow to monitor distance changes on the nanometer scale and in real time [1][2]. FRET Efficiencies are dependent on a number of parameters like the spectral overlap of the donor (D) emission with the absorption of the acceptor dye (A), as well as the distance from and orientation to each other [3].

Up to now, a whole plethora of suitable dye combinations for two-color systems has been reported, but it has turned out that the development of so called three-color or triple FRET (tc-FRET) is much more demanding. A tc-FRET consists of two coupled donor–acceptor pairs sharing one chromophore which acts as a relay station A_1 for the energy transfer from the donor D to the acceptor A_2 (*Fig. 1*).

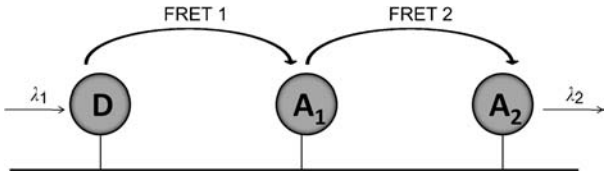

Fig. 1. *Principle of the three-color FRET system*

Such systems offer the advantage that they yield information about the position of the three chromophores relative to each other, they extend the working range

compared to conventional FRET systems, and the spectral shift between the excitation of the donor and the emission of A_2 is much more pronounced. In addition, fewer labeled sample molecules are required to measure relative distances [4][5]. Despite these obvious advantages, relatively few systems have been hitherto reported [6–17]. The main reason for this is the difficulty to identify three chromophores with matching spectroscopic properties as well as the development of suitable chemistry required for their specific incorporation into biomolecules.

We have recently reported on a novel tc-FRET system which we had successfully tested in peptides as well as in synthetic DNA [18]. The system consisted of a carbostyril (=quinolin-2(1*H*)-one)-derived donor D, a [Ru^{II}(bathophenanthroline)] acceptor A_1, and an anthraquinone (=anthracene-9,10-dione) quencher A_2 (bathophenanthroline = 4,7-diphenyl-1,10-phenanthroline). All three chromophores were introduced by a building-block approach avoiding postsynthetic labeling. Additional features of our new system were robustness, outstanding well-matching spectroscopic properties, large *Förster* distances, and high sensitivity. The full set of fundamental photophysical properties was investigated in great detail. The experimental data were in excellent agreement with theoretical calculations that were also performed for this tc-FRET system.

An anthraquinone chromophore served as quencher entity (A_2 in *Fig. 1*) for the Ru complex, and no sensitized emission of the final FRET step was observed. This has, on the one hand, the advantage that the photoluminescence of the Ru complex is not obscured by an emission of the quencher, but it also has, on the other hand, the consequence that no positive signal of A_2 can be observed, which could be of additional analytical benefit, *e.g.*, by increasing the usable spectral shift further into the NIR spectral region.

The aim of this work was to replace the anthraquinone quencher in our original tc-FRET system by an emitting dye. This would lead to a positive, even more red-shifted signal as a result of the second energy transfer. Moreover, if it was possible to transfer a long decay time on this dye, it would have generally implications for such systems. Insertion of a relay chromophore with a distinct longer luminescence emission compared to conventional organic dyes would be enough to turn the system into a position that it can be measured in a time resolved mode with the possibility to largely eliminate any background fluorescence. Since the luminescence of the Ru complex decays on a μs time scale, the decay time characteristics of the dye used as A_2 should be significantly increased, and the application of a time-gated detection scheme in luminescence assays based on this tc-FRET system could be envisioned.

As a suitable chromophore, we have identified the cyanine dye **6** which was synthesized according to the *Scheme* [19]. Thus, 2,3,3-trimethyl-3*H*-indol (**1**) was first treated with 6-bromohexanoic acid (**2**) to form the indolium salt **3**. Upon reaction with the hydrochloride of the bis-imine **4** of malonaldehyde, the hemicyanine was formed which was then treated with indolium salt **5** to yield finally the desired Cy5 derivative **6**.

A comparison of the absorption/emission spectra of the carbostyril-derived donor (D), the Ru complex (Ru), and the Cy5 derivative **6** (Cy) revealed a sufficiently strong overlap between the emission of the Ru complex with the absorption of **6** demonstrating its potential suitability for the aspired tc-FRET system (*Fig. 2*).

Scheme. *Synthesis of Cyanine Dye* **6** (Cy)

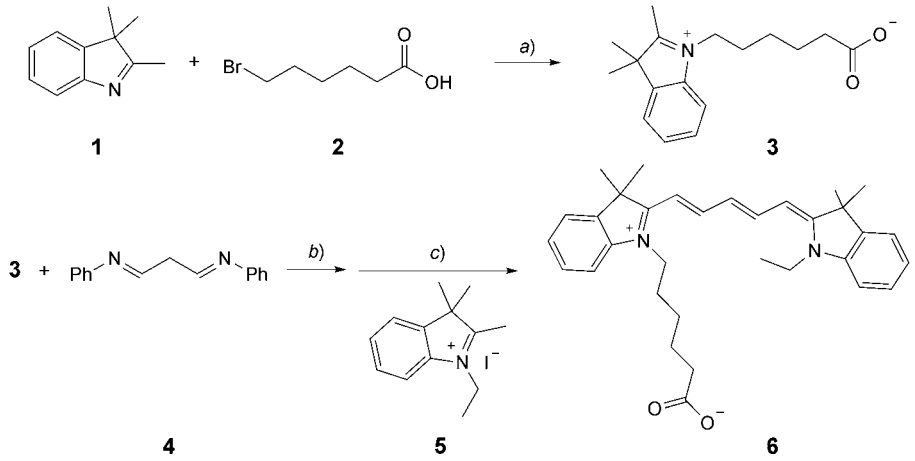

a) Microwave oven (110°, 15 bar max, 50 W), 35 min; 69%. *b*) Ac_2O, 120°, 90 min. *c*) Pyridine, r.t., overnight; yield over 2 steps 85%.

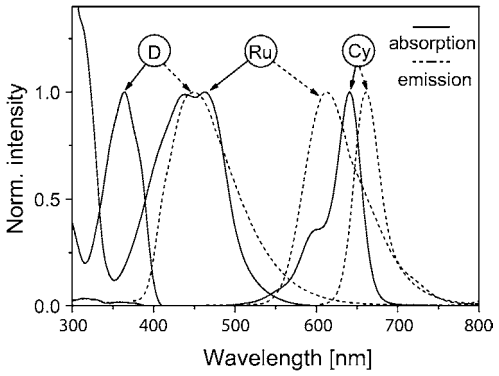

Fig. 2. *Spectral overlaps among the dyes*

Synthetic double-stranded DNA decorated with the chromophores of a FRET system is an ideal tool for the systematic investigation of the latter. It allows to place the chromophores at will into defined positions within the DNA. Furthermore, due to the rigid core structure, the distances between the dyes are controllable and can be varied according to the requirements. In addition, influences based on ground-state interactions hampering the estimation of reliable numerical values characterizing the energy-transfer process (*e.g.*, energy-transfer efficiencies, *Förster* radii) can be minimized. For these obvious reasons, we aspired towards the verification of the new tc-FRET system in DNA *via* the entities outlined in *Fig. 3*.

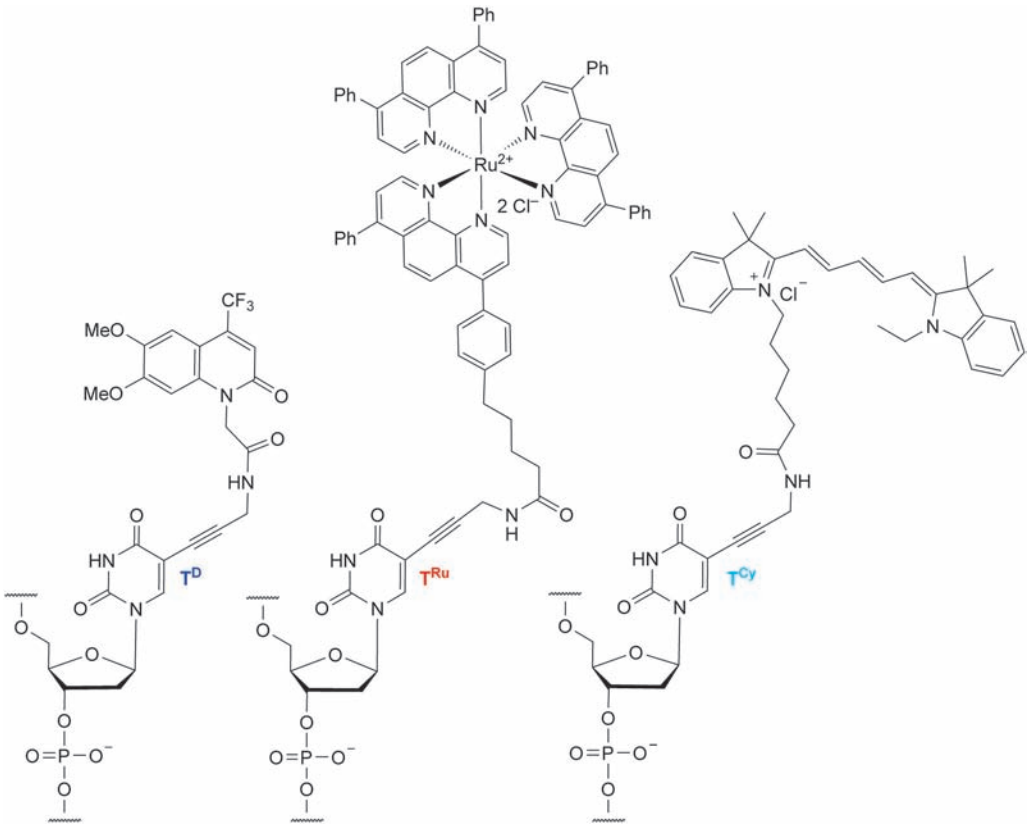

Fig. 3. *Chromophores attached to the DNA*

Results and Discussion. – The incorporation of the carbostyril-derived donor and the [Ru^{II}(bathophenanthroline)] complex was accomplished *via* their phosphoramidites and was described in detail in our previous publication [18]. Preliminary experiments had revealed that cyanine dyes are not perfectly stable under the conditions employed during DNA synthesis. This was unfortunately also true for the Cy5 derivative **6**, so that its incorporation by means of a phosphoramidite building block was doomed to failure. Hence, we had to pursue a postsynthetic labeling. For this purpose, **6** was coupled to an amino-modified synthetic DNA after its release from the support and deprotection *via* an amide function. Purification of the desired DNA fragment after this step was then performed by prep. HPLC on reversed-phase silica gel.

For a detailed biophysical characterization of the new tc-FRET system, the DNA sequences **7**–**17** were required (*Fig. 4*). All sequences containing the Cy5 chromophore were prepared by a postsynthetic labeling procedure, the details of which are outlined in [20]. The unlabeled sequences were the same as those used in our previously reported system. This held also true for the DNA fragment containing the [Ru^{II}(bathophenanthroline)] complex as label.

Fig. 4. *Sequences used for the photophysical investigations*

The tc-FRET system was then established by hybridizing the Ru-complex-modified fragment to the complementary strands equipped with the donor and **6** (Cy) as depicted in *Fig. 5*. The different hybrids were then investigated by photophysical measurements.

The synthesized array of sequences would allow us to characterize double-stranded samples with different relative distances between the donor (D), Ru (A_1), and Cy (A_2). As outlined in the previous publication, the different dyes were in all hybrids well separated, so that significant ground-state interactions, *e.g.*, due to orbital overlap, could be excluded. This also allowed for a nondisturbed investigation of both FRET pairs involved. The first energy-transfer step from D to the Ru complex has already been investigated in detail in our previously described tc-FRET system and compared to other donor derivatives [21].

A comparison of the spectral data of free **6** and the sequences **10** and **11** indicated only minor differences concerning the absorption coefficient as well as the wavelength of the absorption maximum (only a slight bathochromic spectral shift $\Delta\lambda$ of 4 nm). This indicated that between the DNA and incorporated **6** (Cy), no significant ground-state interaction was operative, which has been reported for many other dyes before [22].

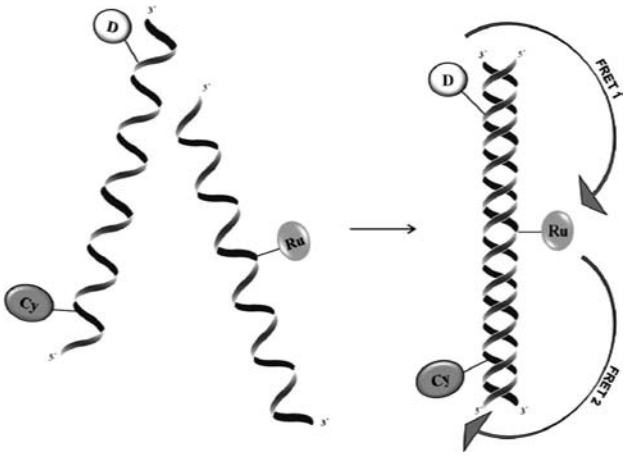

Fig. 5. *Principle of the three-color-FRET DNA arrangement*

The combination between sequence **7** and **10** (Cy_2) or **11** (Cy_1) was used for the study of the second FRET pair consisting of the Ru complex and the cyanine chromophore **6** (Cy). Upon excitation at λ_{ex} 430 nm, sequence **7** revealed the strong emission at λ_{em} 620 nm. After hybridization to **11** (Cy_1), this emission was strongly reduced concomitantly with a strong emission at λ_{em} 665 nm indicative of an effective FRET. This effect was as expected less pronounced for the combination of **7**/**10** due to the greater distance between the two dyes (*Fig. 6*).

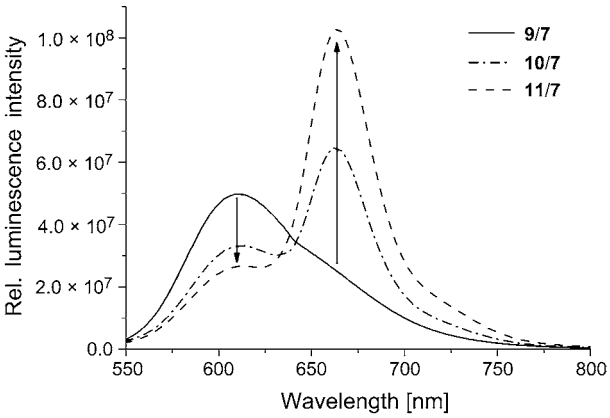

Fig. 6. *Steady-state measurements* (λ_{ex} 430 nm) *of the FRET pair Ru*/*Cy at different distances between them in hybridized DNA strands* (**9**/**7**: no Cy; **10**/**7**: Cy_2; **11**/**7**: Cy_1)

The combination between sequences **12** and **13** with the Ru-complex-labeled DNA fragment **7** was then used to confirm the functionality of the tc-FRET system. This was done in comparison with the combination of sequence **16** and **7** confirming the first

FRET step between the carbostyril-derived donor and the [Ru^{II}(bathophenanthroline)] complex in the presence of Cy and with sequence **16** containing just the donor as a control. Upon excitation at λ_{ex} 360 nm, sample **16** showed a strong emission at λ_{em} *ca.* 440 nm. As expected, this emission was declined in the combination **16**/**7** due to the energy transfer to the Ru complex resulting in the sensitized emission at λ_{em} *ca.* 620 nm. In the tc-FRET arrangement **12**/**7**, this emission was clearly reduced giving rise, at the same time, to an emission at λ_{em} 665 nm (*Fig. 7*), clearly indicative of an active second FRET step. As expected, the tc-FRET was reduced due to the larger distance between the Ru complex and Cy in the sample **13**/**7**.

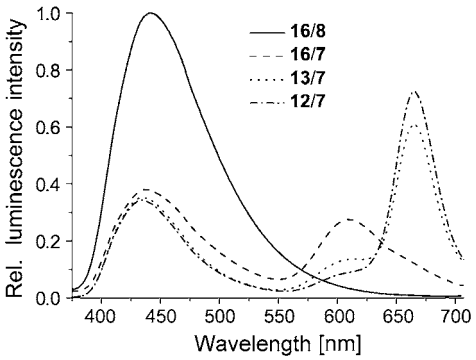

Fig. 7. *Steady-state emission spectra of the FRET constructs in hybridized DNA strands excited at* λ_{ex} *360 nm*

For the determination of the FRET efficiency η, *Eqn. 1* can be used, where I is the luminescence intensity of D in the presence and I_0 in the absence of A. The relationship between the FRET efficiency η and the distance R between D and A can be seen in *Eqn. 2*. With the *Förster* radius R_0 of a given FRET pair and the calculated energy-transfer efficiency, it is possible to determine the spectroscopic distance R^{spec} ($= R$) between D and A.

$$\eta = 1 - \frac{I}{I_0} \tag{1}$$

$$\eta = \left[1 + \left(\frac{R}{R_0}\right)^6\right]^{-1} \leftrightarrow R = R_0\left[\left(\frac{1}{\eta}\right) - 1\right]^{\frac{1}{6}} \tag{2}$$

In the *Table*, the FRET efficiencies are summarized together with the distances between the dyes. The distances R^{theo} obtained from accessible volume (AV) simulations [18] and the R values calculated from FRET data of stationary-emission-intensity measurements were in excellent agreement (see *Table*).

An interesting issue is the dependence of the fluorescence decay time of the Ru complex and the Cy derivative. Changes in fluorescence decay times are of special

Table 1. *FRET Efficiencies Based on Emission Intensity Data and Distances* R *Between the Different Dyes.* Compared are the theoretical and the experimentally determined distances.

	Sample	$\eta_{D/Ru}$	$\eta_{Ru/Cy}$	$R_{D/Ru}^{theo}$ [nm][a])	$R_{Ru/Cy}^{theo}$ [nm][a])	$R_{D/Ru}^{spec}$ [nm][b])	$R_{Ru/Cy}^{spec}$ [nm][c])
17/7	D_2-Ru-	0.22 ± 0.08	–	4.6 ± 0.7	–	4.7 ± 0.5	–
14/7	D_2-Ru-Cy_2	0.23 ± 0.07	0.56 ± 0.06	4.6 ± 0.7	4.3 ± 0.8	4.7 ± 0.4	4.8 ± 0.2
15/7	D_2-Ru-Cy_1	0.26 ± 0.03	0.61 ± 0.05	4.6 ± 0.7	3.8 ± 0.9	4.5 ± 0.1	4.7 ± 0.2
16/7	D_1-Ru-	0.52 ± 0.10	–	3.2 ± 0.5	–	3.8 ± 0.3	–
13/7	D_1-Ru-Cy_2	0.53 ± 0.10	0.53 ± 0.08	3.2 ± 0.5	4.3 ± 0.8	3.7 ± 0.3	4.9 ± 0.2
12/7	D_1-Ru-Cy_1	0.44 ± 0.15	0.66 ± 0.05	3.2 ± 0.5	3.8 ± 0.9	4.0 ± 0.5	4.5 ± 0.2
10/7	-Ru-Cy_2	–	0.51 ± 0.07	–	4.3 ± 0.8	–	5.0 ± 0.2
11/7	-Ru-Cy_1	–	0.68 ± 0.09	–	3.8 ± 0.9	–	4.4 ± 0.3
	Sample	$\eta_{D/Cy}$		$R_{D/Cy}^{theo}$ [nm][a])		$R_{D/Cy}^{spec}$ [nm][d])	
14/8	D_2- -Cy_2	0.11 ± 0.09		7.4 ± 0.7		4.7 ± 0.7	
15/8	D_2- -Cy_1	0.13 ± 0.08		6.4 ± 0.6		4.5 ± 0.7	
13/8	D_1- -Cy_2	0.14 ± 0.08		6.4 ± 0.6		4.5 ± 0.7	
12/8	D_1- -Cy_1	0.21 ± 0.04		4.1 ± 0.7		4.1 ± 0.8	

[a]) Calculated from AV simulations. [b]) With $R_{0(D/Ru)} = 38.2$ Å. [c]) With $R_{0(Ru/Cy)} = 50.0$ Å. [d]) With $R_{0(D/Cy)} = 33.3$ Å.

interest since they are basically independent on the concentration of the fluorophore and, therefore, not prone to any artefacts induced by fluctuations of the concentrations of donor and acceptor. This makes a data evaluation based on decay-time measurements more robust, which is especially beneficial in life-science applications. In *Fig. 8*, the fluorescence decay time of the samples **9/7**, **10/7**, and **11/7** are shown. In the presence of Cy, the fluorescence decay kinetics of the Ru complex were distinctly altered. With decreasing distance between Cy and the Ru complex, an increase in the observed quenching was found (first part of the decay curves of samples **10/7** and **11/7**, resp.). In

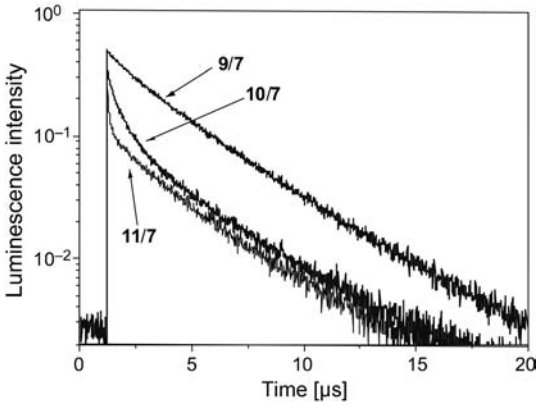

Fig. 8. *Changes in the luminescence decay of the emission at λ_{em} 620 nm of the Ru complex due to the FRET between the Ru complex and Cy dye in hybridized DNA strands* (λ_{ex} 430 nm)

the absence of Cy, a simple luminescence decay of the Ru complex (according to a first-order decay law) was observed. The presence of Cy induced a more complex fluorescence decay kinetics. A tentative explanation for the observed time dependence is the presence of slightly different distances between donor (Ru complex) and acceptor (Cy) during the liftetime of the electronically excited Ru complex, resulting in a distribution of energy transfer efficiencies. Here, work is in progress to analyse the experimental data with more sophisticated decay models considering such a distribution in the distances between the Ru complex and Cy.

A further issue of interest is the influence of the long decay time of the emission of the Ru complex on the fluorescence decay time of Cy. For this investigation, we used again the combination of the sequences **10** and **11** with the Ru-complex-labeled sequence **7**. In *Fig. 9*, the fluorescence decay kinetics of Cy upon indirect excitation (λ_{ex} 430 nm) *via* the Ru complex (and subsequent transfer of energy to Cy by FRET) as well as upon direct excitation (λ_{ex} 590 nm) are shown for the samples **10**/**7** and **11**/**7**. In case of direct excitation of Cy, no difference in the decay kinetics were observed for the two samples. In contrast, for the sensitized excitation, *i*) a distinct change compared to direct excitation, and *ii*) a clear relation to the relative distance between D and A was found. Due to the energy transfer, the long decay kinetics of the Ru complex was 'transferred' to the Cy dye. Like in the well-known systems in which lanthanide complexes (often containing europium or terbium as central ions) are used as donor and the energy is transferred to organic dyes (*e.g.*, in homogeneous fluorescence immuno assays (FIA) [23]), the decay kinetics of the Ru complex was 'punched' on the Cy dye. Based on the information gained in time-resolved fluorescence experiments, contributions from direct *vs.* indirect (equal to successful FRET) could be readily distinguished. Moreover, any fluorescence arising from matrix components that may obscure the measurement could now also be excluded, since those signals are expected to decay on a lower nanosecond timescale. Compared to the lanthanide-based systems commonly used in FIA applications, Ru complexes show higher thermodynamic and (even more important) kinetic stability, which make such FRET systems highly attractive as an alternative for FIA-based diagnostic applications.

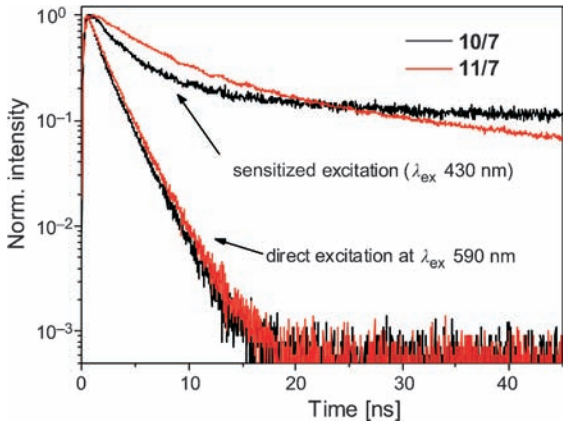

Fig. 9. *Lifetime extension caused by energy transfer* (λ_{em} 670 nm) *in hybridized DNA strands*

Conclusion and Outlook. – We successfully established a novel three-color FRET system consisting of a carbostyril-derived donor, a [Ru^{II}(bathophenanthroline)] complex, which served as a relay chromophore, and a Cy5 derivative as a second acceptor (A_2). With their widely matching spectroscopic properties, the combination of these three chromophores yielded excellent FRET efficiencies with respect to the single as well as the overall transfer step. In contrast to our earlier published tc-FRET system, where a nonfluorescent anthraquinone quencher was employed as A_2, we used in this approach three emitting chromophores. The benefit of such a system is that the FRET efficiency could now also be determined *via* the emission of the third chromophore. Furthermore, the long emission luminescence kinetics of the Ru-complex was transferred to the Cy dye so that the decay time of the Cy chromophore was significantly increased, and the whole tc-FRET system could be measured in a time-resolved mode, virtually free of background, with high sensitivity. The system was established in synthetic DNA as a show case, but it should find general application in interaction studies of biomolecules.

Experimental Part

General. Column chromatography (CC): silica gel *60* (SiO_2; ACC 35–70 μm). UV Spectra: *Perkin-Elmer-Lambda-35* UV/VIS spectrometer. ^{1}H-, ^{13}C-, and ^{31}P-NMR Spectra: *AC 250*, *AM 400*, and *DRX 500* (*Bruker*), and *Mercury VX 300* (*Varian*); $CDCl_3$, CD_3OD, CD_3CN, or (D_6)DMSO as solvent; δ in ppm, *J* in Hz. APCI-MS: *LCQ Advantage* (*Thermo*); APCI = atmospheric-pressure chemical ionization; in *m*/*z* (rel. %).

General Procedures for the Synthesis and Characterization of Oligonucleotides. Oligonucleotide syntheses were carried out on an *Expedite™ 8909* nucleic acid synthesis system on a 1 μmol scale by means of phosphoramidite chemistry and standard protocols. Phosphoramidites as well as nucleosides coupled to solid support (CPG) were obtained from *Proligo*/*Sigma–Aldrich*. Cleavage of the modified and unmodified oligonucleotides from the solid support and concomitant deprotection was performed by adding a 25% NH_3 soln. followed by vortexing overnight at r.t. After exchanging the counter ion NH_4^+ by K^+, the oligonucleotide samples were desalted by size-exclusion chromatography (*NAP-10* column). Purification of the donor- and Ru-complex-labeled oligonucleotides was performed by prep. polyacrylamide-gel electrophoresis (PAGE). Pre-electrophoresis was performed overnight at 400 V with *Tris*/borate buffer. Oligonucleotide (5 μl, 1 *OD*/μl in H_2O) and bromophenol blue/xylenecyanol soln. (5 μl) were heated to 90° for 2 min and rapidly cooled to 0° before being loaded onto the gel. Electrophoretic separation was performed for 18 h at 400 V. The gel was visualized at 366 nm, and the bands containing the desired DNA were isolated and cut into small slices. Together with twice the volume of *MilliQ* water, they were extracted overnight. After centrifugation, the supernatant was collected and concentrated. The resulting donor- and Ru-complex-labeled oligonucleotide samples were desalted by size-exclusion chromatography (*NAP-10* column). Purification of the Cy-labeled oligonucleotides was performed by prep. HPLC (*Merck*/*Hitachi* system, anal. *EC-125*/*4-Nucleosil-100-5-C18* column). The mobile phase was a gradient of solvent *A* (0.1M $Et_3NH(OAc)$ buffer at pH 7.0) and solvent *B* (MeCN).

All oligonucleotides were analyzed by electrophoresis on polyacrylamide gels (20%) of 0.4 mm thickness. Pre-electrophoresis was performed for 2 h at 500 V with *Tris*/borate running buffer. Oligonucleotides (1 μl, 0.1 *OD*/μl in H_2O) and bromophenol blue/xylenecyanol soln. (2 μl) were heated to 90° for 2 min and rapidly cooled to 0° before being loaded onto the gel. Electrophoretic separations were performed for 2 h at 500 V. Oligonucleotide bands were stained with a soln. of 3,3′-diethyl-9-methyl-4,5,4′,5′-dibenzothiacarbocyanine bromide ('Stains All', *Fluka*).

*1-(5-Carboxypentyl)-2,3,3-trimethyl-3*H*-indolium Bromide* (**3**·HBr) [19]. A mixture of 6-bromohexanoic acid (**2**; 670 mg, 3.4 mmol, 1 equiv.) and 2,3,3-trimethyl-3*H*-indol (**1**; 541 mg, 3.4 mmol, 1 equiv.) was irradiated for 35 min. in a microwave oven (110°, 15 bar max, 50 W). Then the mixture was

dissolved in MeCN (3 ml) and the crude product precipitated with Et_2O (50 ml). The obtained crystals were filtered off and purified by CC (SiO_2; 2 → 10% MeOH/CH_2Cl_2): **3**·HBr (739 mg, 69%). Pink crystals. M.p. 122–125° ([19]: 127–129°). Spectroscopic data: in accordance with literature data. ^{1}H-NMR ((D$_6$)DMSO, 400 MHz): 1.41–1.46 (*m*, $COCH_2CH_2CH_2$); 1.51–1.58 (*s*, 2 Me–C(3), $COCH_2CH_2$); 1.80–1.86 (*m*, NCH_2CH_2), 2.22 (*t*, *J*(CH_2,CH_2) = 7.2, $COCH_2CH_2$); 2.85 (*s*, Me–C(2)); 4.46 (*t*, *J*(CH_2,CH_2) = 7.7, NCH_2); 7.61–7.63 (*m*, H–C(5), H–C(7)); 7.84–7.86 (*m*, H–C(6)); 7.96–7.99 (*m*, H–C(4)); 12.00 (br. *s*, NH). ^{13}C-NMR ((D$_6$)DMSO, 100 MHz): 13.98 (Me); 21.97 (CH_2CH_2COOH); 23.98 (Me); 25.38 (Me); 26.90 (NCH_2CH_2); 33.33 (CH_2COOH); 38.87 (C(3)); 54.12 (NCH_2); 115.46 (C(7)); 123.47 (C(4)); 128.90 (C(5)); 129.36 (C(6)); 141.01 (C(8)); 141.84 (C(9)); 174.24 (COOH); 196.48 (C(2)). APCI-MS: 544.9 (8), 272.3 (100, [*M* – Br$^-$]$^+$).

*2-[5-(1-Ethyl-1,3-dihydro-3,3-dimethyl-2*H*-indol-2-ylidene)penta-1,3-dien-1-yl]-3,3-dimethyl-1-(5-carboxypentyl)-3*H*-indolium Chloride* (**6**·HCl) [19]. Compound **3**·HBr (200 mg, 0.53 mmol, 1.00 equiv.) and malonaldehyde bis(phenylimine) monohydrochloride (= *N*,*N*′-propane-1,3-diylidenebis[benzenamine] hydrochloride (1:1); **4**·HCl; 165 mg, 0.57 mmol, 1.10 quiv.) were dissolved in Ac_2O (10 l) and stirred for 30 min at 120°. After cooling to r.t., 1-ethyl-2,3,3-trimethyl-3*H*-indolium iodide (**5**; 234 mg, 0.74 mmol, 1.40 equiv.) in pyridine (10 ml) was added, and the mixture was stirred overnight at r.t. The solvent was evaporated, and the residue dissolved in $CHCl_3$ (8 ml), and the crude product precipitated with hexane (40 ml). The obtained blue crystals were filtered off and then dissolved in $CHCl_3$ (30 ml). The $CHCl_3$ soln. was washed with H_2O (2 × 30 ml) and 0.1M HCl (30 ml), dried ($MgSO_4$), and concentrated and the residue purified by CC (SiO_2, 0 → 10% MeOH/CH_2Cl_2): **6**·HCl (258 mg, 85%). Blue solid. Spectroscopic data: in accordance with literature data. ^{1}H-NMR (CD_3OD, 400 MHz; H_a to H_e = protons of pentadienyl): 1.38 (*t*, *J*(Me,CH_2) = 7.2, *Me*CH_2); 1.45–1.53 (*m*, $COCH_2CH_2CH_2$); 1.64–1.70 (*m*, $COCH_2CH_2$); 1.71–1.74 (2*s*, 2 *Me*–C(3), 2 *Me*–C(3′)); 1.78–1.88 (*m*, NCH_2CH_2); 2.31 (*t*, *J*(CH_2,CH_2) = 7.3, $COCH_2CH_2$); 4.08–4.19 (*m*, 2 NCH_2); 6.29 (*d*, $J_{a,b}$ = 14, H_a); 6.30 (*d*, $J_{e,d}$ = 14, H_e); 6.60–6.68 (*m*, H_c); 7.22–7.31 (*m*, H–C(5), H–C(5′), H–C(7), H–C(7′)); 7.38–7.43 (*m*, H–C(6), H–C(6′)); 7.47–7.50 (*m*, H–C(4), H–C(4′)); 8.20–8.29 (*m*, H_b, H_a). ^{13}C-NMR (CD_3OD, 100 MHz): 12.55; 21.29; 27.36; 27.86; 27.97; 28.15; 34.72; 39.99; 44.80; 50.56; 50.61; 104.05; 104.28; 108.98; 111.81; 112.02; 122.97; 123.41; 123.46; 126.21; 126.28; 126.62; 129.75; 129.78; 142.66; 142.81; 143.08; 143.57; 155.47; 155.63; 174.40; 174.66. ESI-MS: 618.1 (10), 499.2 (6), 498.2 (36), 497.1 (100, [*M* – Cl$^-$]$^+$), 483.2 (11), 482.1 (33), 468.2 (11), 467.2 (35).

Oligonucleotides **7**–**17**. The modified carbostyril donor and the Ru complex were incorporated *via* a pre-synthetic labeling strategy by means of labeled phosphoramidites [18]. For the incorporation of the Cy5 derivative **6** a postsynthetic strategy was applied by using an amino-modified phosphoramidite. All modified building blocks (67 μmol/ml in MeCN) were incorporated into the corresponding oligonucleotide sequences during the automated synthesis by using standard DNA-synthesis cycles.

The coupling of the hydroxysuccinimide (NHS) ester of the Cy5 derivative **6** to the free amino function of the oligonucleotide was carried out in a buffer soln. A stock soln. of the Cy5-NHS ester (10 mg) in DMF (420 μl) was prepared. To the amino-modified DNA (20 *OD*, 60 nmol, in 200 μl of H_2O), 1M $NaHCO_3$ (26 μl, pH 8.5) and 52.5 μl of the Cy5-NHS ester stock soln. were added and incubated for 24 h at r.t. Then 3M AcONa (30 μl) and EtOH (825 μl) were added, and the mixture was incubated on dry ice for 1 h. After centrifugation, the supernatant was decanted, and the residue was washed with cold EtOH (3 × 1 ml) and purified by prep. HPLC (0–100% *B* in 48 min).

Hybridization. To the DNA strands **9**–**17** (0.1 *OD* in 1 μl of H_2O), 1.0 equiv. of the corresponding complementary DNA strand **7** or **8** (0.1 *OD* in 1 μl of H_2O) was added, and the solvent was evaporated. The precipitate was dissolved in phosphate buffer (5 mM, pH 7), and thermal hybridization was performed by heating the sample to 90° for 2 min which was followed by slow cooling to r.t.

Photophysical Characterization. The steady-state absorption and fluorescence measurements were performed on a *Cary-500* UV/VIS spectrometer (*Varian*) and a *Fluoromax3* fluorescence spectrometer (*Jobin Yvon*), resp. The decay curves were measured on a *FL920* fluorescence spectrometer (*Edinburgh Instruments*) in the time-correlated single-photon-counting mode. For the excitation of the Ru^{II} entity, the frequency-doubled output of a titanium–sapphire laser (λ_{ex} 430 nm) was used. The repetition rate of 80.2 MHz was reduced to 50 kHz by a *Pulse Picker* (*Pulse Select*, *APE*). The donor entity was excited with a picosecond-pulsed laser diode *EPL-375* (*Edinburgh Instruments*) at λ_{ex} 375 nm and a repetition

rate of 5 MHz. The excitation of the Cy entity was done with a supercontinuum laser source *SC-400-PP* (*Fianium*) at λ_{ex} 590 nm with a repetition rate of 20 MHz. The sample luminescence was measured in a right-angle configuration to the incoming beam and detected with a multichannel plate (*Europhoton*). In the data evaluation, the fluorescence spectra of Ru^{II} were corrected for the bleed through contribution of the Cy dye.

Calculation of *Förster* radii R_0 was based on the spectroscopic properties of the dyes and performed with *Eqn. 3*, where Φ_D is the quantum yield of the donor, n the refractive index of the solvent, N_A the *Avogadro* number, $F_D(\lambda)$ the area normalized donor emission spectra, $\varepsilon_A(\lambda)$ the extinction coefficient of the acceptor, κ^2 the orientation of the transition dipols of D and A to each other, and λ the wavelength.

$$R_0^6 = \frac{(9 \cdot \ln 10)\kappa^2 \Phi_D}{128\pi^5 n^4 N_A} \int_0^\infty F_D(\lambda)\varepsilon_A(\lambda)\lambda^4 d\lambda \tag{3}$$

Theoretical Calculations. The theoretical interdye distances were calulated by accessible volume (AV) simulations based on the Model Satelite Prior algorithm implemented in the FRETnpsTools program, as discribed in [24][25]. The pdb file of double-stranded DNA was built with the Nucleic Acid Builder (NAB) software provided by AmberTools [26].

REFERENCES

[1] K. E. Sapsford, L. Berti, I. L. Menditz, *Angew. Chem., Int. Ed*. **2006**, *45*, 4562.
[2] P. Tinnefeld, M. Sauer, *Angew. Chem., Int. Ed*. **2005**, *44*, 2642.
[3] T. Förster, *Ann. Phys.* **1948**, *2*, 55.
[4] H. M. Watrob, C.-P. Pan, M. D. Barkley, *J. Am. Chem. Soc*. **2003**, *125*, 7336.
[5] Z.-J. Jiang, W. A. Goedel, *Phys. Chem. Chem. Phys* **2008**, *10*, 4584.
[6] E. Galperin, V. V. Verkhusha, A. Sorkin, *Nat. Methods* **2004**, *1*, 209.
[7] L. He, X. Wu, J. Simone, D. Hewgill, P. E. Lipsky, *Nucleic Acids Res.* **2005**, *33*, e61.
[8] S. Kawahara, T. Uchimaru, S. Murata, *Chem. Commun.* **1999**, 563.
[9] A. K. Tong, S. Jokusch, Z. Li, H.-R. Zhu, D. L. Akins, N. J. Turro, J. Ju, *J. Am. Chem. Soc.* **2001**, *123*, 12923.
[10] A. K. Tong, Z. Li, G. S. Jones, J. J. Russo, J. Ju, *Nat. Biotechnol*. **2001**, *19*, 756.
[11] J. Liu; Y. Lu, *J. Am. Chem. Soc*. **2002**, *124*, 15208.
[12] Y. Ohya, K. Yabuki, M. Hashimoto, A. Nakajima, T. Ouchi, *Bioconjugate Chem.* **2003**, *14*, 1057.
[13] E. Haustein, M. Jahnz, P. Schwille, *ChemPhysChem* **2003**, *4*, 745.
[14] S. Hohng, C. Joo, T. Ha, *Biophys. J.* **2004**, *87*, 1328.
[15] J.-P. Clamme, A. A. Deniz, *ChemPhysChem* **2005**, *6*, 74.
[16] P. Tinnefeld, M. Heilemann, M. Sauer, *ChemPhysChem* **2005**, *6*, 217.
[17] I. H. Stein, V. Schüller, P. Böhm, P. Tinnefeld, T. Liedl, *ChemPhysChem* **2011**, *12*, 689.
[18] A. Kienzler, R. Flehr, R. A. Kramer, S. Gehne, M. U. Kumke, W. Bannwarth, *Bioconjugate Chem.* **2011**, *22*, 1852.
[19] M. V. Kvach, A. V. Ustinov, I. A. Stepanova, A. D. Malakhov, M. V. Skorobogatyi, V. V. Shmanai, V. A. Korshun, *Eur. J. Org. Chem.* **2008**, 2107.
[20] L. Clima, C. Hirtz-Haag, A. Kienzler, W. Bannwarth, *Helv. Chim. Acta* **2007**, *90*, 1082.
[21] R. A. Kramer, R. Flehr, M. Lay, M. U. Kumke, W. Bannwarth, *Helv. Chim. Acta* **2009**, *92*, 1933.
[22] A. Kupstat, T. Ritschel, M. U. Kumke, *Bioconjugate Chem.* **2011**, in press.
[23] N. Hildebrandt, L. J. Charbonnière, M. Beck, R. F. Ziessel, H.-G. Löhmannsröben, *Angew. Chem., Int. Ed*. **2005**, *44*, 7612.
[24] A. Muschielok, J. Andrecka, A. Jawhari, F. Brückner, P. Cramer. and J. Michaelis, *Nat. Methods* **2008**, *5*, 965; A. Muschielok, J. Michaelis, FRETnps Tool 2.6, 2008, Ludwig-Maximilians-Universität Munich.

[25] S. Sindbert, S. Kalinin, H. Nguyen, A. Kienzler, L. Clima, W. Bannwarth, B. Appel, S. Müller, C. A. M. Seidel, *J. Am. Chem. Soc.* **2011**, *133*, 2463.

[26] D. A. Case, T. A. Darden, I. T. E. Cheatham, C. L. Simmerling, J. Wang, R. E. Duke, R. Luo, R. C. Walker, W. Zhang, K. M. Merz, B. Roberts, B. Wang, S. Hayik, A. Roitberg, G. Seabra, I. Kolossváry, K. F. Wong, F. Paesani, J. Vanicek, X. Wu, S. R. Brozell, T. Steinbrecher, H. Gohlke, Q. Cai, X. Ye, M. J. Hsieh, G. Cui, D. R. Roe, D. H. Mathews, M. G. Seetin, C. Sagui, V. Babin, T. Luchko, S. Gusarov, A. Kovalenko, P. A. Kollman, AmberTools Version 1.4, 2010, University of California, San Francisco.

Received November 21, 2011